Incorporation of an Energy Equation into a Pulsed Inductive Thruster Performance Model

Kurt A. Polzin
NASA-Marshall Space Flight Center, Huntsville, AL 35812, USA

Jarred P. Reneau
Mississippi State University, Starkville, MS 39762, USA

Kameshwaran Sankaran
Whitworth University, Spokane, WA 99251, USA

kurt.a.polzin@nasa.gov

I. INTRODUCTION

Pulsed inductive plasma accelerators are electrodeless space propulsion devices where a capacitor is charged to an initial voltage and then discharged through a coil as a high-current pulse that inductively couples energy into the propellant. The field produced by this pulse ionizes the propellant, producing a plasma near the face of the coil. Once a plasma is formed if can be accelerated and expelled at a high exhaust velocity by the Lorentz force arising from the interaction of an induced plasma current and the magnetic field. While there are many coil geometries that can be employed to inductively accelerate a plasma, in this paper the discussion is limit to planar geometries where the coil take the shape of a flat spiral. A recent review of the developmental history of planar-geometry pulsed inductive thrusters can be found in Ref. [1]. Two concepts that have employed this geometry are the Pulsed Inductive Thruster (PIT)[2, 3] and the Faraday Accelerator with Radio-frequency Assisted Discharge (FARAD)[4].

There exists a 1-D pulsed inductive acceleration model that employs a set of circuit equations coupled to a one-dimensional momentum equation. The model was originally developed and used by Lovberg and Dailey[2, 3] and has since been nondimensionalized and used by Polzin *et al.*[5, 6] to define a set of scaling parameters and gain general insight into their effect on thruster performance. The circuit presented in Fig. 1 provides a description of the electrical coupling between the current flowing in the thruster I_1 and the plasma current I_2. The acceleration model is limited, however, because it lacks a time-accurate description of the energy in the plasma, relying instead on an assumed, constant electron temperature T_e. While this does permit the computation of a plasma resistivity, that resistivity value cannot vary in time. Additionally, various energy sink descriptions cannot be included in the model without an equation that accurately describes the energy in the system.

In this paper we revise the pulsed inductive acceleration model to calculate the energy in the plasma as a function of time. This will permit the plasma temperature and commensurate pressure to vary throughout the duration of the current pulse. It will also provide a path for the inclusion of more complex energy dissipation models (plasma radiation, two-temperature modeling, etc.) without requiring computations through much more complicated two- and three-dimensional magnetohydrodynamic simulations. The energy equation is used to compute the deposition of power into various modes. One example of these calculations is presented in Fig. 2. The model

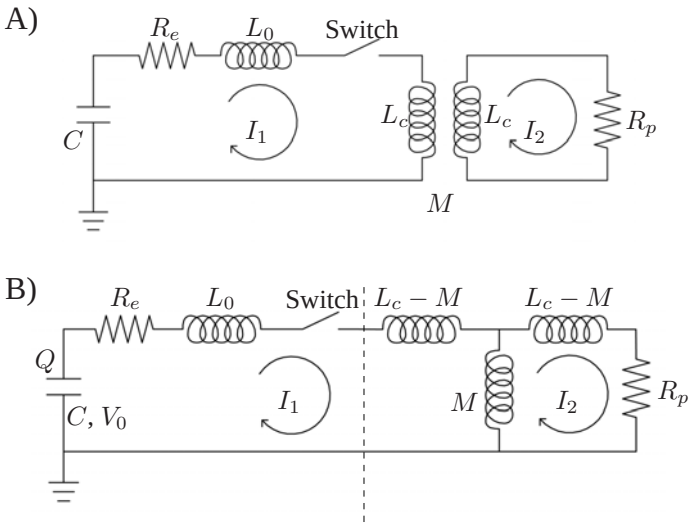

FIG. 1: A) General lumped element circuit model of a pulsed inductive accelerator. B) Equivalent electrical circuit model. (After Ref. [2])

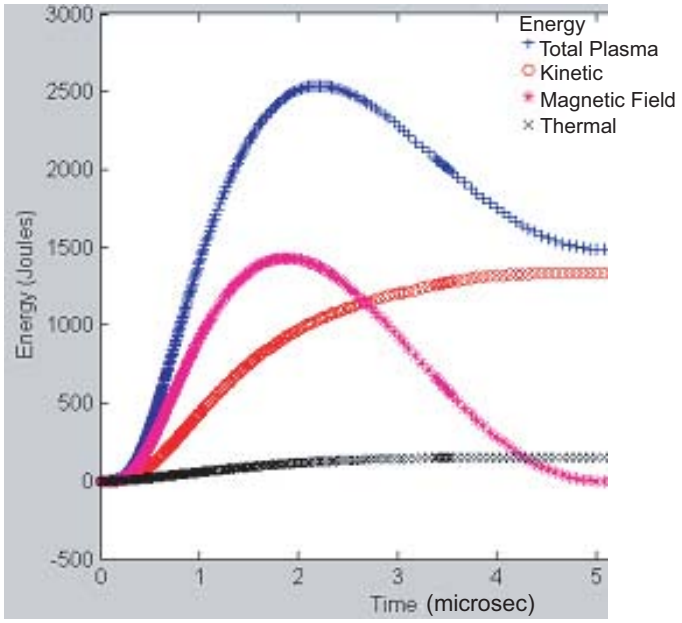

FIG. 2: Calculated time-history of the total plasma energy and each component of energy.

is compared to the case that assumes T_e is constant to show the benefits of including the energy equation in the calculation.

[1] K.A. Polzin, "Comprehensive review of planar pulsed inductive plasma thruster research and technology," *J. Propuls. Power*, **in press**, 2011.

[2] R.H. Lovberg and C.L. Dailey, "Large inductive thruster performance measurement," *AIAA J.*, **20**(7):971, 1982.

[3] C.L. Dailey and R.H. Lovberg, "The PIT MkV Pulsed Inductive Thruster," TRW Systems Group, Tech. Rep. NASA CR-191155, Jul. 1993.

[4] E.Y. Choueiri and K.A. Polzin, "Faraday Accelerator with Radio-Frequency Assisted Discharge (FARAD)," *J. Propuls. Power*, **22**(3):611, 2006.

[5] K.A. Polzin and E.Y. Choueiri, "Performance optimization criteria for pulsed inductive plasma acceleration," *IEEE Trans. Plasma Sci.*, **34**(3):945, 2006.

[6] K.A. Polzin, Faraday Accelerator with Radio-Frequency Assisted Discharge (FARAD), Ph.D. Dissertation, 3147-T, Princeton Univ., Princeton, NJ, 2006.

Incorporation of an Energy Equation into a Pulsed Inductive Thruster Performance Model

IEPC-2011-181

Presented at the 32nd International Electric Propulsion Conference, Wiesbaden, Germany
September 11-15, 2011

Kurt A. Polzin*
NASA-Marshall Space Flight Center, Huntsville, AL 35812, USA

Jarred P. Reneau†
Mississippi State University, Starkville, MS 39762, USA

Kameshwaran Sankaran‡
Whitworth University, Spokane, WA 99251, USA

A model for pulsed inductive plasma acceleration containing an energy equation to account for the various sources and sinks in such devices is presented. The model consists of a set of circuit equations coupled to an equation of motion and energy equation for the plasma. The latter two equations are obtained for the plasma current sheet by treating it as a one-element finite volume, integrating the equations over that volume, and then matching known terms or quantities already calculated in the model to the resulting current sheet-averaged terms in the equations. Calculations showing the time-evolution of the various sources and sinks in the system are presented to demonstrate the efficacy of the model, with two separate resistivity models employed to show an example of how the plasma transport properties can affect the calculation. While neither resistivity model is fully accurate, the demonstration shows that it is possible within this modeling framework to time-accurately update various plasma parameters.

I. Introduction

Pulsed inductive plasma accelerators are electrodeless space propulsion devices where a capacitor is charged to an initial voltage and then discharged through a coil as a high-current pulse that inductively couples energy into the propellant. The field produced by this pulse ionizes the propellant, producing a plasma near the face of the coil. Once a plasma is formed if can be accelerated and expelled at a high exhaust velocity by the Lorentz force arising from the interaction of an induced plasma current and the magnetic field. While there are many coil geometries that can be employed to inductively accelerate a plasma, in this paper the discussion is limit to planar geometries where the coil take the shape of a flat spiral. A recent review of the developmental history of planar-geometry pulsed inductive thrusters can be found in Ref. [1]. Two concepts that have employed this geometry are the Pulsed Inductive Thruster (PIT)[2,3] and the Faraday Accelerator with Radio-frequency Assisted Discharge (FARAD).[4]

There exists a 1-D pulsed inductive acceleration model that employs a set of circuit equations coupled to a one-dimensional momentum equation. The model was originally developed and used by Lovberg and Dailey[2,3] and has since been nondimensionalized and used by Polzin *et al.*[5,6] to define a set of scaling parameters and gain general insight into their effect on thruster performance. The circuit presented in Fig. 1 provides a description of the electrical coupling between the current flowing in the thruster I_1 and the

*Propulsion Research Engineer, Propulsion Research and Technology Applications Branch, Propulsion Systems Department. kurt.a.polzin@nasa.gov

†Graduate Research Assistant, NASA-Graduate Student Research Program (GSRP) Fellow.

‡Associate Professor, Physics Department.

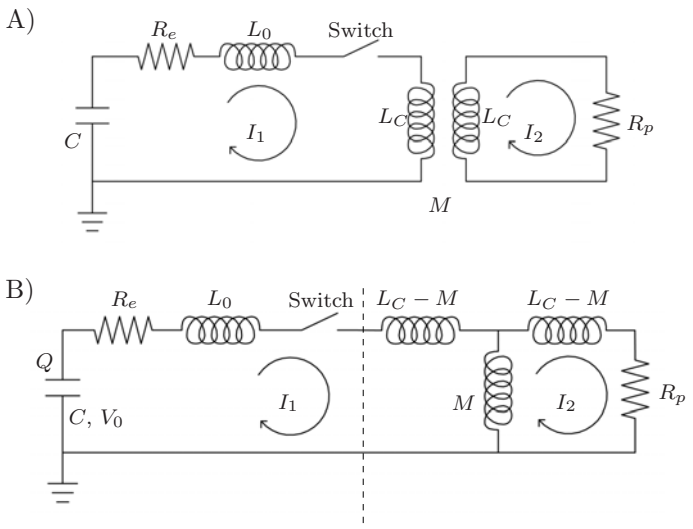

Figure 1. A) General lumped element circuit model of a pulsed inductive accelerator. B) Equivalent electrical circuit model. (After Ref. [2])

plasma current I_2. The acceleration model is limited, however, because it lacks a time-accurate description of the energy in the plasma, relying instead on an assumed, constant electron temperature T_e. While this does permit the computation of a plasma resistivity, that resistivity value cannot vary in time. Additionally, various energy sink descriptions cannot be included in the model without an equation that accurately describes the energy in the system.

In this paper we revise the pulsed inductive acceleration model to calculate the energy in the plasma as a function of time. This will permit the plasma temperature and commensurate pressure to vary throughout the duration of the current pulse. It will also provide a path for the inclusion of more complex energy dissipation models (plasma radiation, two-temperature modeling, etc.) without requiring computations using much more complicated two- and three-dimensional magnetohydrodynamic simulations.

II. Governing Equations

We proceed with a presentation of the equations governing the response of a pulsed inductive accelerator, discussing in turn the circuit model, plasma acceleration model, energy equation, and plasma model.

A. Electrical Circuit Model

The lumped-element circuit model of a pulsed inductive accelerator presented in Fig. 1A is redrawn in Fig. 1B so as to permit the application of Kirchoff's law to the two current loops. The external circuit (left side of the figure) possesses capacitance C, external inductance L_0, resistance R_e, and acceleration coil inductance L_C. The plasma also has an inductance equal to L_C and a resistance R_p. The two circuits are inductively coupled through the acceleration coil, which acts as a transformer with mutual inductance M. The value of M is a function of the current sheet position z. The time-varying behavior of this circuit is governed by the following coupled set of first-order ordinary differential equations:

$$\frac{dI_1}{dt} = \frac{V\,L_C + (MI_1 + I_2L_C)\,(dM/dt) - I_2MR_p - I_1R_eL_C}{L_C\,(L_0 + L_C) - M^2}, \tag{1}$$

$$\frac{dI_2}{dt} = \frac{M\ (dI_1/dt) + I_1\ (dM/dt) - I_2R_p}{L_C}, \tag{2}$$

$$\frac{dV}{dt} = -\frac{I_1}{C} \tag{3}$$

where V is the voltage on the capacitor.

Following Lovberg and Dailey,[7] the total inductance of the system can be written as

$$L_{\text{tot}}(z) = L_0 + L_p(z) \tag{4}$$

where L_p is the position-varying portion (called herein the plasma inductance), which is equal to the total inductance presented to the circuit by the circuit elements on the right side of the dashed line in Fig. 1B. Based on experimental measurements, it has been found that the plasma inductance as a function of axial current sheet position can be modeled as

$$L_p(z) = L_C\left(1 - \exp\left(-\frac{z}{z_0}\right)\right) \tag{5}$$

where z_0 is defined as the electromagnetic decoupling length. Another way to think of L_p is as the approximate Thevenin equivalent plasma inductance to the right of the dashed line in Fig. 1B.

The series and parallel inductances in the system can be approximately combined into one total inductive element with the value

$$L_{\text{tot}} = L_0 + \left(L_C - \frac{M^2}{L_C}\right). \tag{6}$$

By equating the terms in the parentheses with the plasma inductance L_p, we find that the mutual inductance is given as

$$M = L_C \exp\left(-\frac{z}{2z_0}\right). \tag{7}$$

The preceding equation can be differentiated to yield

$$\frac{dM}{dt} = -\frac{L_C}{2z_0}\exp\left(-\frac{z}{2z_0}\right)\frac{dz}{dt}. \tag{8}$$

which governs the time-varying behavior of the mutual inductance and completes the set of circuit equations.

B. Plasma Acceleration Model

The current sheet, shown schematically in Fig. 2, is modeled as a plasma slab moving with velocity v_z into an ambient neutral gas. The mass of propellant accumualted by the current sheet is m, the thickness of the current sheet is δ_a, and the temperature, pressure, and ratio of specific heats inside the plasma are given as T_{cs}, p_{cs}, and γ_{cs}, respectively. Ambient neutral gas conditions in front of the sheet are denoted with the subscript A and are given for the density ρ_A, pressure p_A, temperature T_A, and ratio of specific heats γ_A. The sheet is assumed to entrain all the gas it encounters, leaving vacuum conditions behind the plasma. The plasma spatially approximated is a disk possessing an inner radius a and an outer radius b, corresponding to the inner and outer radii of the acceleration coil.

The equations of motion are generally similar to those given in Ref. [7], but they have been rederived from first principles, specifically including the pressure gradient term in the momentum equation. The equation for mass accumulation can be found by assuming one-dimensional motion and integrating the MHD equation for conservation of mass over the sheet volume to obtain

$$\frac{dm}{dt} = \rho_A(z)\, v_z \quad \text{where } \rho_A(z) = \begin{cases} \rho_0\,(1 - z/\delta_m) \\ 0 \end{cases} \tag{9}$$

where the assumed mass distribution in front of the current sheet is triagular. The linear mass density ρ_0 corresponding to this distribution is given as $2(m_{\text{bit}} - m_0)/\delta_m$ where m_{bit} is the total propellant mass in the pulse and m_0 is the initial mass in the current sheet. Assuming a value for the ambient temperature T_A, the pressure p_A can be found using the ideal gas equation of state

$$p_A = \frac{\rho_A}{\pi\,(b^2 - a^2)}\frac{k_B}{M}T_A \tag{10}$$

where k_B is Boltzmann's constant and M is the atomic or molecular mass.

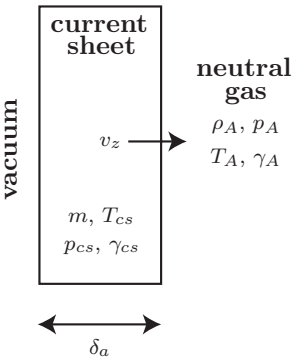

Figure 2. Schematic showing the variables used to describe conditions within and just outside the current sheet.

The momentum equation for the current sheet is found by assuming one-dimensional motion and integrating the MHD momentum equation over the current sheet volume, resulting in

$$\frac{dv_z}{dt} = \left[\frac{L_c I^2}{2z_0}\exp\left(-\frac{z}{z_0}\right) - \rho_A(z)\, v_z^2 - p_A \pi\left(b^2 - a^2\right)\right]/m(t) \tag{11}$$

where the final term on the right hand side containing p_A arises from the pressure gradient term in the momentum equation.

C. Energy Equation

In previous work the system of equations was closed[7] by assuming that the plasma temperature T was constant. The value of this constant was left as a free parameter and varied to produce agreement between the model and experimental data. An even more simplified closure approximation that was used in Ref. [5] is to assume R_p is a constant.

To properly model the time-varying energy distribution in the plasma we begin with the MHD equation governing the evolution of the energy density in the system, given as[8]

$$\frac{\partial \varepsilon}{\partial t} + \nabla \cdot \left[(\varepsilon + p)\,\mathbf{v} - \bar{\bar{B}}_M \cdot \mathbf{v}\right] = \nabla \cdot \left(\frac{-\mathbf{E}' \times \mathbf{B}}{\mu_0}\right) \tag{12}$$

where ε the energy density defined as

$$\varepsilon = \frac{p}{\gamma - 1} + \frac{1}{2}\rho v^2 + \frac{B^2}{2\mu_0}.$$

The first term on the right hand side in the definition of ε is the internal energy density of the plasma, the second term is the gas kinetic energy density, and the third term is the magnetic field energy density. In Eq. (12), the term on the right side is Ohmic heating, the term $\nabla \cdot \left(\bar{\bar{B}}_M \cdot \mathbf{v}\right)$ is the electromagnetic work, the term $\nabla \cdot (\varepsilon \mathbf{v})$ is the net convection of power into a control volume, and $\nabla \cdot (p\mathbf{v})$ represents the pressure work performed against the current sheet per unit time.

We previously observed that the plasma inductance in Eq. 5 is the approximately equal to the Thevenin-equivalent inductance to the right of the dashed line in Fig. 1B. If we could find a Thevenin-equivalent resistance R_p', then the voltage drop across the plasma (i.e. across the two points intersected by the dashed line) is

$$V_p = R_p I + \dot{\phi}(t) = R_p' I_1 + L_p \frac{dI_1}{dt} + I_1 \frac{dL_p}{dt} \quad \text{(magnetic flux } \phi = L_p I\text{)}. \tag{13}$$

Multiplying by I_1 yields the total power into the plasma as:

$$P = \frac{d}{dt}\left(\frac{L_p I_1^2}{2}\right) + \frac{I_1^2}{2}\frac{dL_p}{dt} + I_2^2 R_p \tag{14}$$

where the first term on the right is the rate of change of the magnetic field energy, the second term is the rate of electromagnetic work performed, and the third term is resistive heating with the Thevenin-equivalent resistive term $I_1^2 R_p'$ replaced by the actual resistive power load $I_2^2 R_p$. For completeness, the time evolution of L_p is governed by the equation

$$\frac{dL_p}{dt} = \frac{L_c}{z_0}\exp\left(-\frac{z}{z_0}\right)\frac{dz}{dt}. \tag{15}$$

To use Eq. (12) in the model, the equation must be integrated over the current sheet volume to obtain an equation for the total plasma energy E. Doing this transforms the time-differential as

$$\frac{\partial \varepsilon}{\partial t} \rightarrow \frac{dE}{dt}.$$

The electromagnetic power term in Eq. (12) is easily replaced using the electromagnetic work term in Eq. (14), resulting in

$$-\nabla \cdot \left(\bar{\bar{B}}_M \cdot \mathbf{v}\right) \rightarrow -\frac{I_1^2}{2}\frac{dL_p}{dt} = -\frac{L_c I_1^2}{2z_0}\exp\left(-\frac{z}{z_0}\right) v_z$$

To integrate the term on the right hand side, we must assume that $\mathbf{E}' = \eta\mathbf{j}$ and that $\mathbf{j}$ is curl free, allowing this term to transform into the resistive power in the current sheet,

$$\nabla \cdot \left(\frac{-\mathbf{E}' \times \mathbf{B}}{\mu_0} \right) \rightarrow I_2^2 R_p$$

The power density convected into the current sheet is

$$\nabla \cdot (\varepsilon \mathbf{v}) \rightarrow \left[\frac{1}{2}\rho_A v_z^2 + \frac{p_A}{\gamma_A - 1}\pi \left(b^2 - a^2\right) \right] v_z - \frac{d}{dt}\left(\frac{L_p I_1^2}{2} \right)$$

where the first term on the right represents the power lost in accelerating entrained gas to the sheet speed, the second term is the net internal power in the entrained gas convecting into the current sheet, and the third term is the time rate-of-change of the electromagnetic field energy as given in Eq. (14). The remaining term from Eq. (12) is the work-per-unit-time performed by the ambiant gas pressure against the face of the current sheet, and is given as

$$\nabla \cdot (p\mathbf{v}) \rightarrow p_A \pi \left(b^2 - a^2\right) v_z$$

Bringing all the transformations above together yields an energy equation for the system as

$$\frac{dE}{dt} = \frac{L_c I_1^2}{2z_0} \exp\left(-\frac{z}{z_0}\right) v_z + I_2^2 R_p + \frac{d}{dt}\left(\frac{L_p I_1^2}{2} \right) - \left[\frac{1}{2}\rho_A v_z^2 + \frac{\gamma_A p_A}{\gamma_A - 1}\pi \left(b^2 - a^2\right) \right] v_z \tag{16}$$

After every timestep, the current sheet pressure p_{cs} can be updated using the relation

$$E = \frac{p_{cs}}{\gamma_{cs} - 1}\delta_a \pi \left(b^2 - a^2\right) + \frac{1}{2} m v_z^2 + \frac{L_p I_1^2}{2} \tag{17}$$

where γ_{cs} is the specific heat ratio for the plasma (assumed equal to 5/3). Once p_{cs} is found, the current sheet temperature can be approximately computed using an ideal gas equation of state to obtain

$$T_{cs} = \frac{p_{cs}}{(1 + Z)\, n_e k_B} \tag{18}$$

where k_B is Boltzmann's constant, Z is the ionization fraction (equal to one assuming a singly-ionized gas) and n_e is the electron number density given (for $Z = 1$) as $(m/M)/(\delta_a \pi \left(b^2 - a^2\right))$ where M is the atomic or molecular mass of the ions. The temperature is used in the subsequent section to obtain the plasma resistivity and other temperature-dependent plasma properties.

D. Plasma Model

Following Ref. [7], we can model the plasma as a finite width slab that grows in time. The plasma resistivity can be simply given using the Spitzer resistivity,

$$\eta(t) = 6 \times 10^{-4} T_{cs}^{-3/2} \quad \text{ohm-m } (T_{cs} \text{ in eV}). \tag{19}$$

An improved (and more realistic) way to find the resistivity is to calculate it directly using collision cross sections to obtain a more accurate function of η as a function of T_{cs}. In Fig. 3 are plotted a Spitzer resistivity and an improved resistivity function that to an extent captures the non-monotonic behavior of an argon gas. We emphasize that the improved resistivity curve depicted in the figure is NOT truly accurate and is only meant to serve as an example of how more realistic resistivity modeling can be incorporated into the system, demonstrating how it affects the resulting calculations.

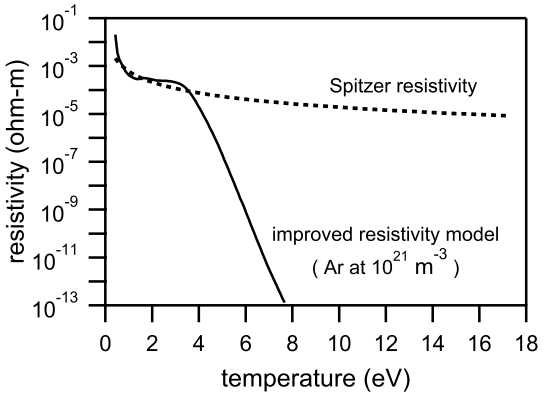

Figure 3. Comparison of the Spitzer resistivity and an improved resistivity model (from Ref. [8] for an argon gas.

The current sheet thickness δ_a has an initial, finite value δ_s at time $t = 0$ and is then assumed to grow on the timescale of resistive diffusion, yielding a time evolution in current sheet thickness as

$$\delta_a(t) = \left(\delta_s^2 + \frac{\eta}{\mu_0} t\right)^{1/2} \tag{20}$$

where μ_0 is the magnetic permeability. For a plasma ring having an outer radius b, an inner radius a, and a thickness $\delta_a(t)$, the total plasma resistance is

$$R_p(t) \approx \frac{\pi \eta(t)\,(b+a)}{\delta_a(t)\,(b-a)}. \tag{21}$$

III. Plasma Simulations

The complete differential equation set given in the previous section consists of Eqs. (1), (2), (3), (8), (9), (11), (15), and (16). These differential equations, together with the supporting equations and models for temperature, pressure, and resistivity, can be solved for a set of initial conditions. In the following section solutions to the equation set are presented for various plasma conditions to demonstrate how the energy is partitioned into different modes by the new energy equation.

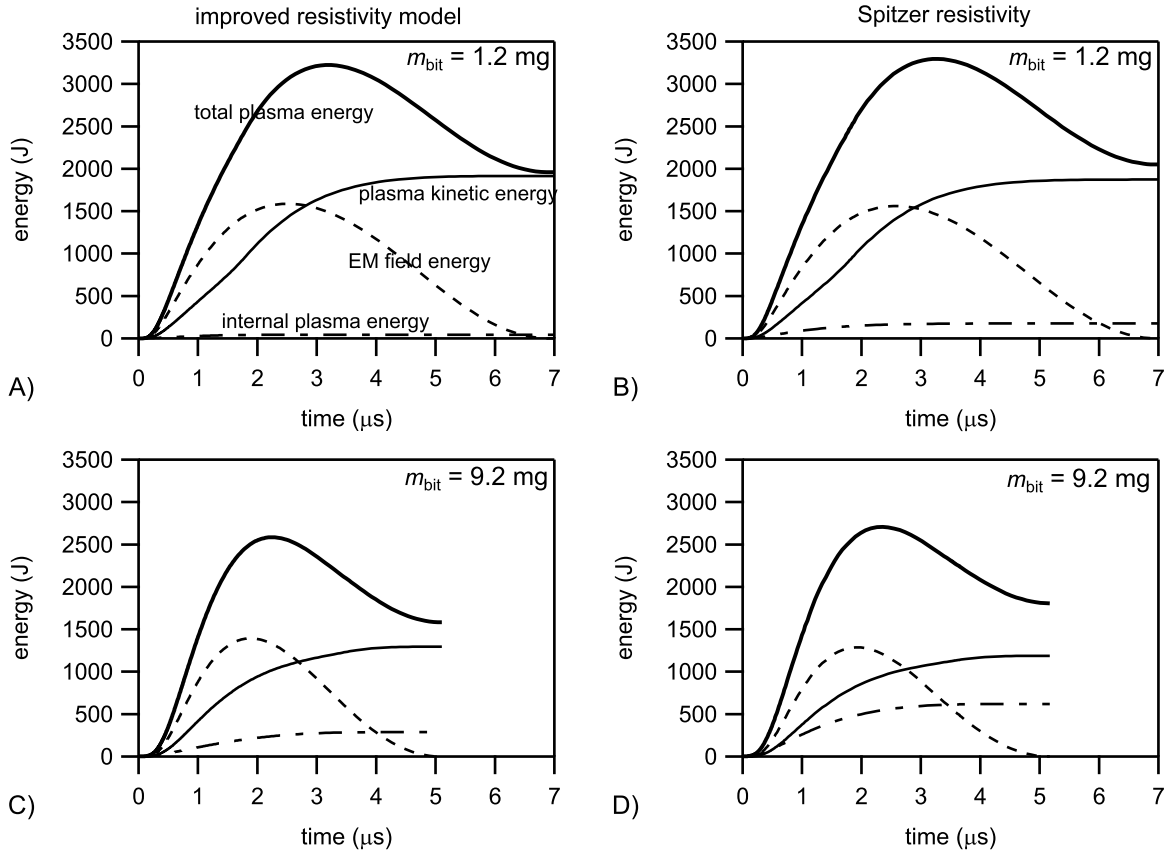

Figure 4. Results of calculations with the acceleration model showing the energy distribution in a pulsed inductive system. The results on the left were generated using the improved resistivity function in Fig. 3 while the results on the right correspond to the use of a Spitzer resistivity. The mass bits for each case are given.

In general, the conditions for the simulations are as follows. The electrial properties employed are similar to the PIT MkVA.[3] The values of L_0 and L_C are 80 nH and 660 nH, respectively, while the value of z_0 is 7.5 cm. The capacitance of the bank is 9 μF and it is charged to 30 kV per pulse. The external resistance of the circuit R_e is 5 mΩ, and the specific heat ratios are all 5/3. The inner and outer radii of the plasma, a and b, are 20 and 50 cm, respectively, and the ambiant gas is assumed to have a temperature of 300 K.

The time histories of various calculated energy sinks in a pulsed inductive thruster are presented in Fig. 4, with results obtained using the improved resistivity model presented in 4A,C and those obtained using a Spitzer resistivity in 4B,D. In all cases, the calculation is terminated at the end of the first half-cycle of the discharge when the current I_1 passes through zero.

In every graph, the total plasma energy is given as the bold solid line. The total energy is split according to Eq. (17) into three components; the internal plasma energy, the electromagnetic field energy, and the plasma kinetic energy. The evolution of all three components are given in each graph, summing to the total plasma energy.

We observe that the first half-cycle period is longer for the lower mass bit cases. The internal plasma energy is greater for the higher mass bit cases, implying significantly increased heating. In addition, the overall energy into the system is greatly reduced in the higher mass bit case owing to poor matching between the external driving circuit and the natural acceleration timescale for the propellant (poorly matched dynamic impedance[5]).

The energy distribution time-histories for the two resistivity models are similar, with slightly increased internal plasma energy at the expense of plasma kinetic energy in the Spitzer resistivity case. However, from Fig. 5 we find that this difference translates into a large difference in the plasma temperature. The 'knee' feature observed in the improved resistivity model appears to regulate and limit the maximum plasma temperature. At lower temperatures, resistive heating tends to increase the temperature, but as the resistivity drops precipitously, the plasma heats very little. In the Spitzer model, there is no 'knee' or inflection point, so the resistive heating rate remains high for a much greater temperature range until the gas decouples from the coil. The initial plasma temperature for all these cases was 4.4 eV. However, simulations using the improved resistivity model at a mass bit of 1.2 mg/pulse revealed that after a short transient all temperature time histories collapsed to the same curve for an initial temperature range from 0.95 eV to 9.5 eV.

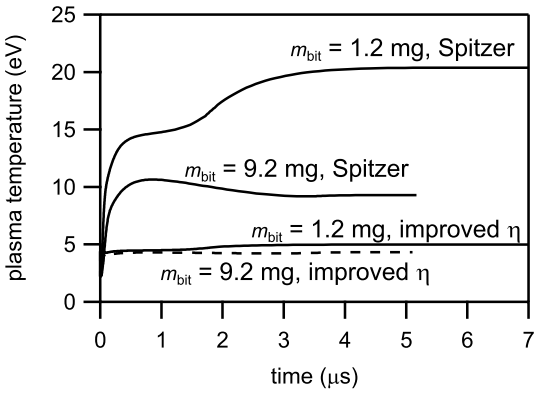

Figure 5. Time-evolution of the plasma temperature for simulations using the Spitzer and improved resistivity models from Fig. 3. The mass bits for each case are given.

IV. Future Work

It cannot be emphasized enough that while the framework for the energy equation developed in this paper is sound, the computations are not yet expected to quantitatively match experimental data. While the resistivity model is an improvement over the Spitzer model, it is still not an exact model of the plasma resistivity and was used herein to demonstrate that there is an effect on the overall energy distribution in the system when a different resistivity model is employed.

Future work will involve the calculation of several plasma parameters in a more self-consistent and time-varying manner. These parameters include the ionization fraction Z, obtained from a Saha relation; the plasma temperature, obtained using a real gas equation of state; and the plasma specific heat ratio γ_{cs}. Fortunately, if these data are tabulated then a table lookup can be developed to update these terms in the equation set. The resistivity can be found using collision cross section information, calculating it from the cross sections for collisions between electrons and every other heavy species in the plasma (neutral, ion, double ion, etc.). The completion of this process will permit the customizing of the acceleration model to a given propellant type, which is not possible without first having an energy equation incorporated into the system of equations.

V. Conclusions

We have presented presented a pulsed inductive plasma acceleration model that includes an energy equation to model the various energy sources and sinks in the system. The MHD equations were integrated over the plasma volume by assuming one-dimensional fluid motion and treating the current sheet as a one-element finite volume. This method generally recovered the equations of motion presented in previous work, with the addition of minor corrective terms. More importantly, it permitted the casting of the MHD energy equation into terms that were already calculated in the acceleration model, allowing for the time evolution of plasma pressure and, through an equation of state, plasma temperature. Results were obtained showing the relative sizes of the energy sinks when a Spitzer resistivity and an improved resistivity were used, demonstrating that the change in the form of the resistivity as a function of temperature did have an effect. While the improved resistivity model is not completely accurate for the plasma, it does show how parameters such as the resistivity, ionization fraction, and specific heat ratio, and a real gas equation of state can be implemented into future modeling efforts.

References

[1]K.A. Polzin, "Comprehensive review of planar pulsed inductive plasma thruster research and technology," *J. Propuls. Power*, **27**(3):513, 2011.

[2]R.H. Lovberg and C.L. Dailey, "Large inductive thruster performance measurement," *AIAA J.*, **20**(7):971, 1982.

[3]C.L. Dailey and R.H. Lovberg, "The PIT MkV Pulsed Inductive Thruster," TRW Systems Group, Tech. Rep. NASA CR-191155, Jul. 1993.

[4]E.Y. Choueiri and K.A. Polzin, "Faraday Accelerator with Radio-Frequency Assisted Discharge (FARAD)," *J. Propuls. Power*, **22**(3):611, 2006.

[5]K.A. Polzin and E.Y. Choueiri, "Performance optimization criteria for pulsed inductive plasma acceleration," *IEEE Trans. Plasma Sci.*, **34**(3):945, 2006.

[6]K.A. Polzin, Faraday Accelerator with Radio-Frequency Assisted Discharge (FARAD), Ph.D. Dissertation, 3147-T, Princeton Univ., Princeton, NJ, 2006.

[7]R.H. Lovberg and C.L. Dailey, "A PIT Primer," RLD Associates, TR005, Lebanon, PA, 1994.

[8]K. Sankaran, Simulation of Plasma Flows in Self-Field Lorentz Force Accelerators, Ph.D. Dissertation, 3121-T, Princeton Univ., Princeton, NJ, 2005.

Incorporation of an Energy Equation into a Pulsed Inductive Thruster Performance Model

32nd International Electric Propulsion Conference
IEPC Paper 2011-181

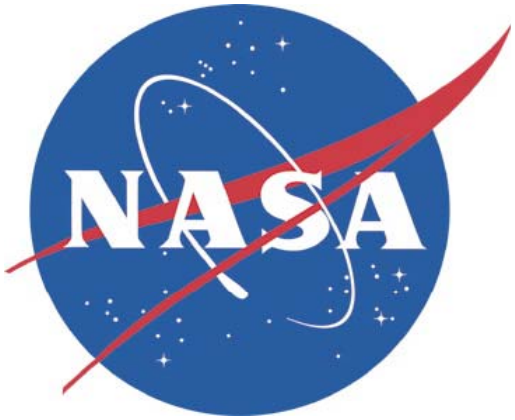

Kurt Polzin
NASA-Marshall Space Flight Center

Jarred Reneau
Mississippi State University

Kameshwaran Sankaran
Whitworth University

Circuit Model

- Pulsed Inductive Thruster circuit coupled to the plasma

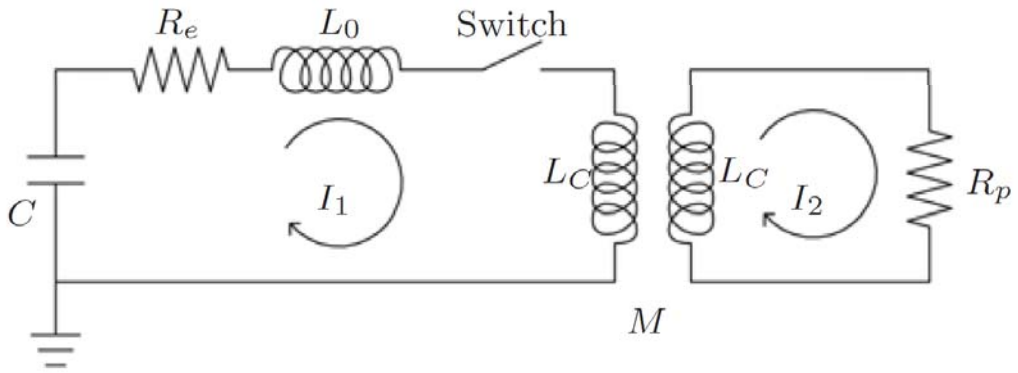

- Pulsed Inductive Thruster equivalent circuit

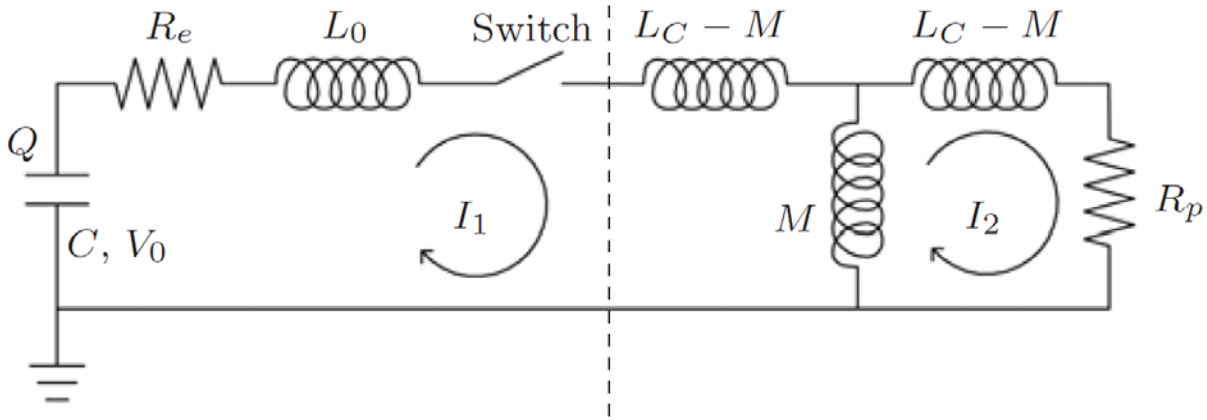

Circuit Equations

- Current, Voltage equations

$$\frac{dI_1}{dt} = \frac{V\,L_C + (MI_1 + I_2L_C)\,(dM/dt) - I_2MR_p - I_1R_eL_C}{L_C\,(L_0 + L_C) - M^2},$$

$$\frac{dI_2}{dt} = \frac{M\ (dI_1/dt) + I_1\ (dM/dt) - I_2R_p}{L_C},$$

$$\frac{dV}{dt} = -\frac{I_1}{C}$$

- System Inductance

$$L_{\mathrm{tot}}\,(z) = L_0 + L_p\,(z) \qquad L_p\,(z) = L_C\left(1 - \exp\left(-\frac{z}{z_0}\right)\right)$$

- Mutual Inductance

$$M = L_C \exp\left(-\frac{z}{2z_0}\right) \qquad \frac{dM}{dt} = -\frac{L_C}{2z_0}\exp\left(-\frac{z}{2z_0}\right)\frac{dz}{dt}$$

Plasma Acceleration Model

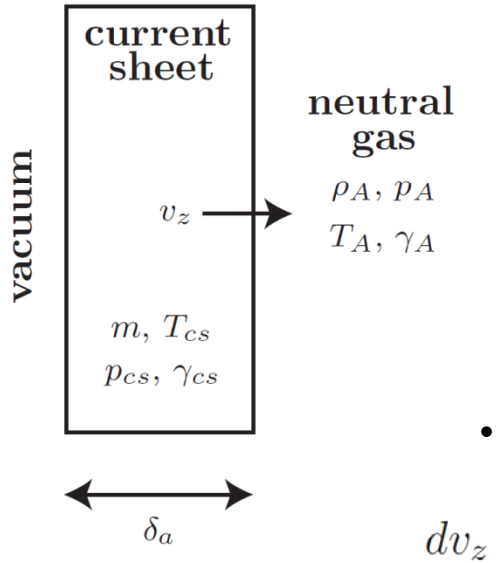

- Continuity Equation

$$\frac{dm}{dt} = \rho_A(z)\, v_z \quad \text{where } \rho_A(z) = \begin{cases} \rho_0 (1 - z/\delta_m) \\ 0 \end{cases}$$

- Conservation of Momentum Equation

$$\frac{dv_z}{dt} = \left[\frac{L_c I^2}{2 z_0} \exp\left(-\frac{z}{z_0}\right) - \rho_A(z)\, v_z^2 - p_A \pi \left(b^2 - a^2\right) \right] / m(t)$$

$$p_A = \frac{\rho_A}{\pi (b^2 - a^2)} \frac{k_B}{M} T_A$$

Energy Equation Formulation

- Energy density evolution equation

$$\frac{\partial \varepsilon}{\partial t} + \nabla \cdot \left[(\varepsilon + p)\,\mathbf{v} - \bar{\bar{B}}_M \cdot \mathbf{v} \right] = \nabla \cdot \left(\frac{-\mathbf{E}' \times \mathbf{B}}{\mu_0} \right)$$

- Energy density

$$\varepsilon = \frac{p}{\gamma - 1} + \frac{1}{2}\rho v^2 + \frac{B^2}{2\mu_0}$$

- Power into plasma from external circuit

$$V_p = R_p I + \dot{\phi}\,(t) = R_p' I_1 + L_p \frac{dI_1}{dt} + I_1 \frac{dL_p}{dt} \quad \text{(magnetic flux } \phi = L_p I\text{)}$$

$$P = \frac{d}{dt}\left(\frac{L_p I_1^2}{2} \right) + \frac{I_1^2}{2}\frac{dL_p}{dt} + I_2^2 R_p$$

- Time-evolution of the plasma inductance

$$\frac{dL_p}{dt} = \frac{L_c}{z_0} \exp\left(-\frac{z}{z_0} \right) \frac{dz}{dt}$$

Energy Equation Formulation

$$\frac{\partial \varepsilon}{\partial t} + \nabla \cdot \left[(\varepsilon + p)\,\mathbf{v} - \bar{\bar{B}}_M \cdot \mathbf{v} \right] = \nabla \cdot \left(\frac{-\mathbf{E}' \times \mathbf{B}}{\mu_0} \right)$$

- Integrating over the current sheet volume and replacing terms with available quantities

Time-rate of change of energy

$$\frac{\partial \varepsilon}{\partial t} \rightarrow \frac{dE}{dt}$$

Resistive heating

$$\nabla \cdot \left(\frac{-\mathbf{E}' \times \mathbf{B}}{\mu_0} \right) \rightarrow I_2^2 R_p$$

Electromagnetic work

$$-\nabla \cdot \left(\bar{\bar{B}}_M \cdot \mathbf{v} \right) \rightarrow -\frac{I_1^2}{2}\frac{dL_p}{dt} = -\frac{L_c I_1^2}{2z_0} \exp\left(-\frac{z}{z_0}\right) v_z$$

Gas entrainment

Magnetic field energy change

$$\nabla \cdot (\varepsilon \mathbf{v}) \rightarrow \left[\frac{1}{2}\rho_A v_z^2 + \frac{p_A}{\gamma_A - 1}\pi\left(b^2 - a^2\right) \right] v_z - \frac{d}{dt}\left(\frac{L_p I_1^2}{2} \right)$$

Internal energy flux

Pressure work on control volume

$$\nabla \cdot (p\mathbf{v}) \rightarrow p_A \pi \left(b^2 - a^2\right) v_z$$

Energy Equation

- New energy equation

$$\frac{dE}{dt} = \frac{L_c I_1^2}{2z_0} \exp\left(-\frac{z}{z_0}\right) v_z + I_2^2 R_p + \frac{d}{dt}\left(\frac{L_p I_1^2}{2}\right) - \left[\frac{1}{2}\rho_A v_z^2 + \frac{\gamma_A p_A}{\gamma_A - 1}\pi\left(b^2 - a^2\right)\right] v_z$$

- Total energy in system

$$E = \frac{p_{cs}}{\gamma_{cs} - 1}\delta_a \pi\left(b^2 - a^2\right) + \frac{1}{2}mv_z^2 + \frac{L_p I_1^2}{2}$$

- Temperature (ideal gas equation of state)

$$T_{cs} = \frac{p_{cs}}{(1+Z)\, n_e k_B}$$

Plasma Models

- Resistivity (Spitzer)

$$\eta(t) = 6 \times 10^{-4} T_{cs}^{-3/2} \quad \text{ohm-m } (T_{cs} \text{ in eV})$$

- Resistivity (improved model)
  - Caution: not truly accurate, for illustrative purposes

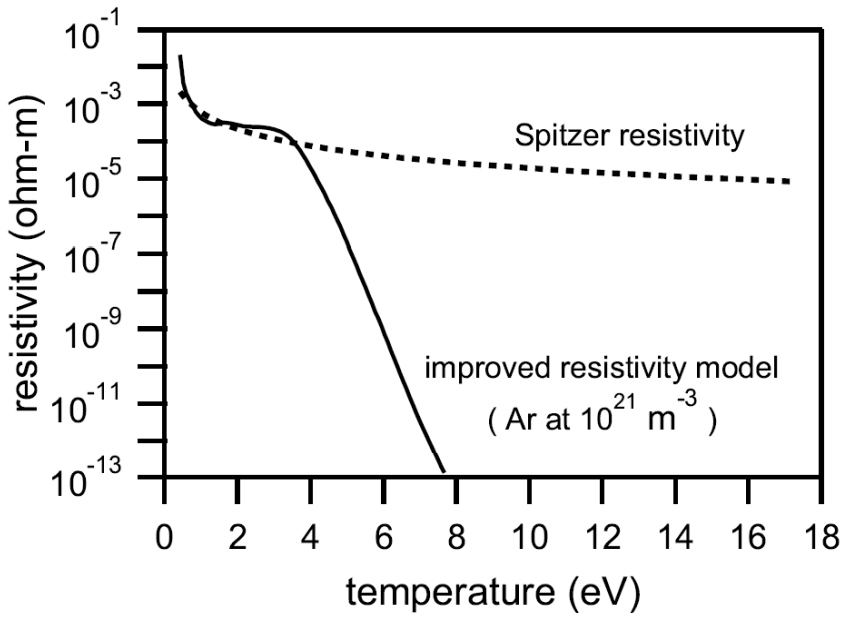

- Current sheet growth

$$\delta_a(t) = \left(\delta_s^2 + \frac{\eta}{\mu_0} t\right)^{1/2}$$

- Plasma resistance

$$R_p(t) \approx \frac{\pi \eta(t)\,(b+a)}{\delta_a(t)\,(b-a)}$$

Plasma Simulations

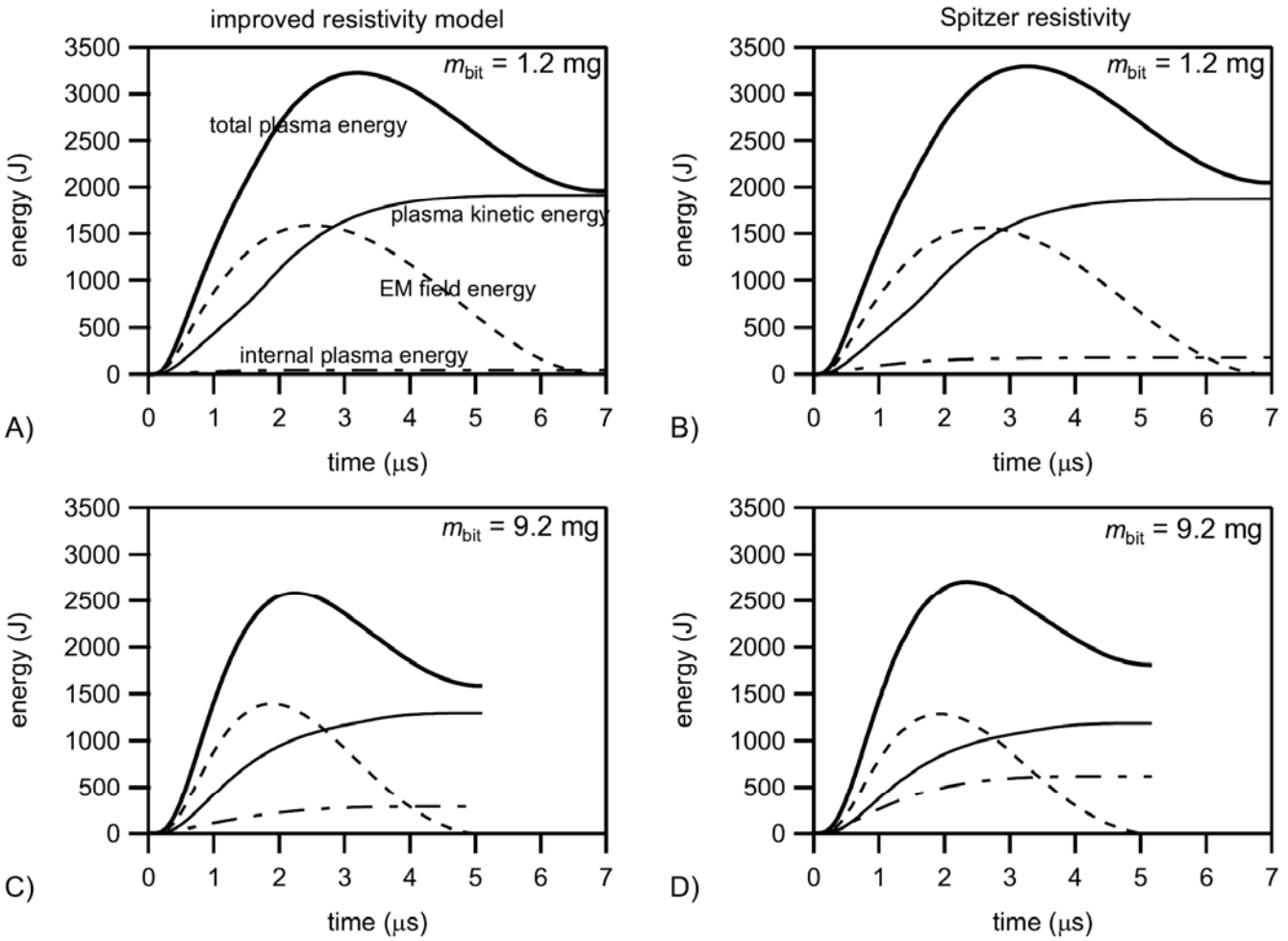

Poorer dynamic impedance matching

More energy into internal plasma heating

Plasma Simulations

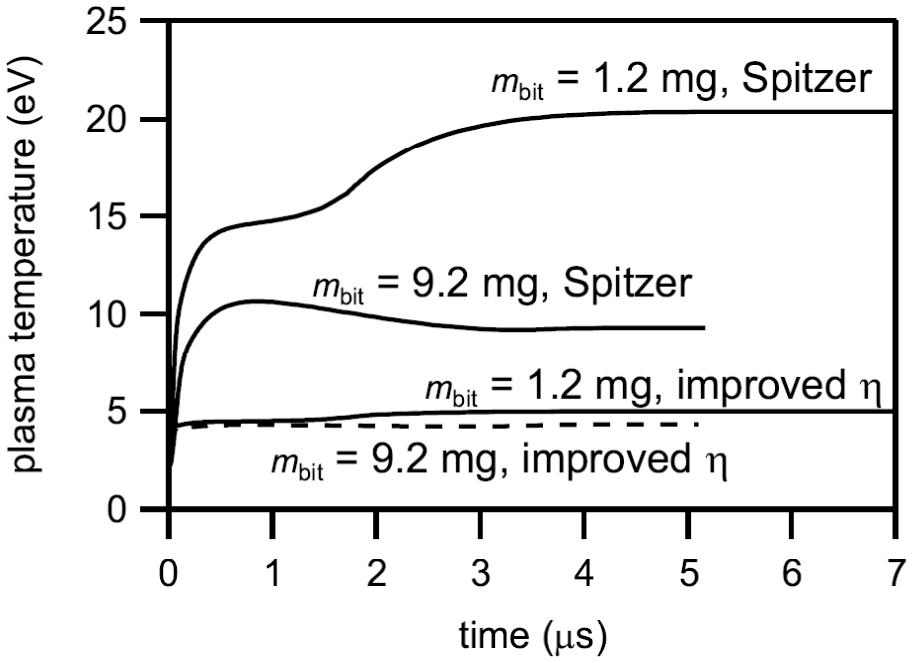

- Much higher temperature for Spitzer resistivity model
- Improved resistivity model self-regulates the temperature about the 'knee' in the resistivity vs. temperature graph
  - Colder plasma → higher η → more heating
  - Hotter plasma → much lower η → less heating
- Improved resistivity model temperatures stabilize to the same value for a wide range of initial temperatures (at least 0.95-9.5 eV)

Future Work

- Fully self-consistent resistivity model calculated using collisional cross sections for electon impact with multiple heavy species including: neutral, ion, double ion, etc.
- Coupling to models for ionization fraction (Saha), real gas equation of state, non-ideal specific heat ratio
- Permits customization of the acceleration model to a specific propellant type

Acknowledgements

- We appreciate and acknowledge the continued MSFC support of Mr. J. Boise Pearson, Mr. James Martin and Ms. Mary Beth Koelbl.

- Jarred Reneau's efforts on this work were supported under a NASA-Graduate Student Research Program (GSRP) fellowship

- This work was supported by NASA's Advanced In-Space Propulsion program managed by Dr. Michael LaPointe.